



OPEN Genomic and metabolomic insights into the antimicrobial compounds and plant growth-promoting potential of *Bacillus velezensis* B115

Jili Chen^{1,7}✉, Yuzhou Feng^{2,7}, Junchi Ma^{1,7}, Qing Zhang¹, Yumei Dong¹, Dongjie Li³, Xuemei Duan⁴, Lequn Zhou⁴, Zhihua Li⁴, Ying Yang⁵, Bo Cai⁵, Ze Liu⁵, Jialong Yu⁶, Bo Zhou⁵✉ & Tao Liu¹✉

The B115 strain, isolated from the inter-root soil of healthy plants in a continuous cropping site of *Panax notoginseng*, was identified as *Bacillus velezensis* B115 by 16S rDNA sequence comparison and comparative genomic analysis. B115 is a strain of beneficial microorganisms present in the inter-root zone of plants, with favorable plant growth-promoting properties and antagonistic effects against the plant pathogen *Fusarium oxysporum*. However, the whole genome of B115 remains unclear, thus restricting its potential applications. To address this gap, the whole genome of B115 has been sequenced and annotated to elucidate the molecular mechanisms underlying its plant growth-promoting and antimicrobial activities. The genome analysis revealed that B115 comprises a single circular chromosome of 4,200,774 bp and a plasmid region 16,878 bp long, possessing a GC content of 45.95%. Moreover, 4349 protein-coding genes were predicted. Notably, the B115 genome contains a substantial number of genes (103) involved in the biosynthesis, transport, and catabolism of secondary metabolites. Through genome mining, 13 BGCs and 540 genes encoding secondary metabolites with predicted roles were identified, including members of the surfactin and fengycin families. Utilizing LC–MS/MS technologies, 2318 metabolites were detected in the fermentation broth of *B. velezensis* B115, encompassing compounds such as Corynebactin, Gamabufotalin, Pracinostat, Indoleacetic acid, (8)-Gingerol, Luteolin, Liquiritigenin, and other metabolites with antimicrobial, growth-promoting, antioxidant, and antitumor properties. By exploring secondary metabolite-related genes and predicting potential secondary metabolites from the B115 genome based on the whole-genome sequence results, we further elucidate the genomic basis for its ability to promote plant growth and inhibit pathogen activity.

Keywords Genome mining, *Bacillus velezensis*, B115, Genes, Secondary metabolites, Genome

Panax notoginseng, a renowned traditional Chinese medicinal herb of the ginseng family (Araliaceae), is a perennial plant^{1,2}, known for enhancing hemostasis and blood circulation³. The roots of *P. notoginseng* have significant medicinal value, often used as raw materials in traditional Chinese medicine⁴. However, during many years of cultivation, *P. notoginseng* can suffer from root rot. *Fusarium oxysporum*, a primary pathogenic fungus responsible for *P. notoginseng* root rot, causes severe developmental retardation, leaf chlorosis, root rot, and necrosis, resulting in substantial economic losses in *P. notoginseng* cultivation^{5,6}. Currently, chemical pesticides are the primary method for managing root rot, but their excessive use poses environmental and agricultural safety

¹College of Agronomy and Biotechnology, Yunnan Agricultural University, Kunming 650201, China. ²College of Resources and Environment, Yunnan Agricultural University, Kunming 650201, China. ³Raw Material Center of China Tobacco Yunnan Industrial Co., Ltd., Kunming 650201, Yunnan, China. ⁴Tobacco Leaf Quality Inspection Section, Raw Material Department, Hongyun Honghe Tobacco (Group) Co., Ltd., Kunming 650201, China. ⁵Technology Center of China Tobacco Yunnan Industrial Co., Ltd., Kunming 650201, Yunnan, China. ⁶Yunnan Tobacco Company, Kunming 650051, China. ⁷Jili Chen, Yuzhou Feng and Junchi Ma contributed equally to this work. ✉email: 2332710778@qq.com; 878343635@qq.com; yantao618@126.com

risks^{7,8}. Biological control offers a promising alternative, with various microbial biological control agents (BCAs) developed for fungal and bacterial disease management⁹. Studies have shown the efficacy of microbial strains in disease control. For instance, Wang et al. demonstrated that inoculating *B. velezensis* B19 in continuous cropping soil of *P. notoginseng* significantly decreased the incidence of root rot in *P. notoginseng* seedlings¹⁰. Kimotho et al. revealed the potential of the endophytic fungus *Purpureocillium lilacinum* YZ1 in controlling *Fusarium* disease in field-grown wheat, promoting growth and enhancing yield¹¹. Furthermore, Dong et al. identified *Bacillus* sp. KW6 and *Lysobacter* sp. KW8 from the inter-root soil of diseased *P. notoginseng* plants with potent antagonistic activity against *F. oxysporum*, notably observing the strongest inhibitory effect at a *Bacillus* sp. KW6 inoculum concentration of 10^8 CFU⁶. Another study showed that *B. velezensis* WB could induce systemic resistance to *Fusarium* wilt in watermelon and reduce the incidence and severity of *Fusarium* wilt in watermelon¹².

Bacillus can thrive in diverse environments and is extensively distributed in nature, particularly in inter-root and plant root systems^{13,14}. In recent years, *Bacillus velezensis* has received increasing attention for its profound inhibitory effects on fungi and bacteria. Not only does it enhance plant growth and inhibit plant pathogens, but it also plays a crucial role in controlling soil-borne diseases^{15,16}. Its mode of action involves the synthesis of phytohormones, solubilization of inorganic phosphate, nitrogen fixation, and acting as an antagonist to soil-borne pathogenic bacteria to foster plant growth. Furthermore, *B. velezensis* protects plants from pathogens assaults by stimulating the production of secondary metabolites related to induced systemic resistance (ISR), which are biologically active against various plant pathogens. The production of *B. velezensis* secondary metabolites is the main cause of its biocontrol activity, such as polyketides compounds including difficidin, bacillaene, and macrolactin. And cyclic lipopeptide compounds including surfactin, fengycin, bacillibactin, iturin, and bacillomycin. Certain compounds, such as fengycin and macrolactin, can serve as fungicides, suppressing plant pathogens and inducing systemic acquired resistance in plants^{17,18}.

Under continuous cropping conditions, *P. notoginseng* shows a serious replant problem, with poor growth and low survival rate, which can lead to serious economic losses¹⁹. Rhizobacteria and endophytic bacteria play important roles in protecting host plants from infection by phytopathogens²⁰. *Bacillus velezensis* B115, was isolated from the inter-root soil of healthy plants in a continuous cropping set of *P. notoginseng*, exhibits growth-promoting qualities and effective antagonistic behavior against *F. oxysporum* as validated by plate assays. In previous study demonstrated that *B. velezensis* B115 may have potential for plant growth promotion, antimicrobial and disease resistance in agriculture and the environment. Although recognized as a promising biocontrol agent, the whole genome of B115 remains inadequately explored, limiting its broader application. Whole genome sequencing can provide a more comprehensive understanding of strains at the genetic level, and genomic analysis of plant beneficial microorganisms can contribute to understanding the biological regulatory mechanisms of biocontrol strains^{21,22}. Previous studies reported the whole genome sequence of *B. velezensis* FZB42 and analyzed its genes encoding antimicrobial compounds, emphasising that microbial compounds have biological control of plant pathogens^{23–25}. Wang et al. conducted an in-depth study on *B. velezensis* Q-426 using whole-genome sequencing, and mined genes related to secondary metabolites from the Q-426 genome, and combined with non-targeted metabolomics to explore the production potential of secondary metabolites of the strain²⁶. In summary, whole genome sequencing can contribute to a more comprehensive understanding of the technical characteristics and safety of strains at the genetic level, help to reveal the bioregulatory mechanisms of biocontrol strains, and provide valuable information to advance the field of microbiological applications²¹.

In this study, culturable strain B115 was isolated from the inter-root soil of healthy plants in a continuous cropping site of *P. notoginseng* and exhibited good antagonistic ability against *F. oxysporum*, as well as possessing plant growth-promoting activity. The taxonomic classification of B115 was ascertained through whole genome sequencing methodologies, construction of a phylogenetic tree utilizing 16S rDNA analysis, and comparative genomic analysis. Furthermore, leveraging genome mining, we identified gene clusters responsible for secondary metabolite biosynthesis in B115, subsequently integrating with non-targeted metabolomics approaches to profile the antimicrobial metabolites present in the strain's fermentation broth. This research seeks to establish a diverse repository of microbial strains for combating root-rot disease in *P. notoginseng* and enhancing plant growth, promising to pave the way for further extensive investigations into the associated genes and their functionalities.

Materials and methods

Molecular characterization of B115

The molecular characterization was done based on 16S rDNA gene sequencing²⁷. The universal primer 27F (5'-A GAGTTTGATCCTGGCTCAG-3') and 1492R (5'-TACGGCTACCTTGTTACGACTT-3') were designed and synthesized. The reaction was performed in 25 μ L reaction volume containing 12.5 μ L of 2 \times Phanta Flash Master Mix (Dye Plus), 2 μ L total genomic DNA, 2 μ L of 27F(5'-AGAGTTTGATCCTGGCTCAG-3') and 2 μ L 1492R (5'-TACGGTTACCTTGTTACGACT-3') of 10 pmol/ μ L, and 6.5 μ L of ddH₂O. PCR was performed using an initial denaturation of 2 min at 98 °C, followed by 30 cycles of 98 °C for 10 s, 55 °C for 30 s and 72 °C for 10 s and final elongation of 72 °C for 1 min in T100 Thermal Cycler (Bio-Rad). PCR product was analyzed on 1% agarose gel prepared in 1 \times TAE buffer. The agarose gel was observed in a gel imaging system. The PCR product was subjected to agarose gel electrophoresis, and were then sent to Sangon Biotech (Shanghai) Co., Ltd. for sequencing.

Bacterial strain and genomic DNA preparation

A strain of *B. velezensis* B115 was isolated from the soil of healthy plants in *P. notoginseng* continuous cropping site in the early stage of our research group. B115 was cultured in Luria–Bertani (LB) medium at 28 °C for 20 h. Subsequently, the cells were harvested by centrifugation at 10,000 rpm for 30 min at 4 °C. High-quality genomic DNA was extracted from strain B115 utilizing a modified CTAB method. The purity (OD260/280 and OD260/230 ratios), concentration, and nucleic acid absorption peaks of the genomic DNA were assessed using Nanodrop.

The genomic DNA concentration was precisely quantified using Qubit 3.0 (Life Technologies, Carlsbad, CA, USA). Furthermore, the Qubit concentration was cross-referenced with the Nanodrop concentration to verify sample purity. Finally, the integrity of the genomic DNA was tested using 0.8% agarose gel electrophoresis.

Genome sequencing and assembly

Use DNA of satisfactory purity, concentration and integrity for use in building library. The library fragment size was detected with an Agilent 2100 Bioanalyzer (Agilent Technologies, USA). Subsequently, the B115 DNA was sequenced via a PacBio Sequel II sequencer, and the generated data were processed with SMRT LINK 10.1.0 software. PacBio reads were reassembled using microbial assembly (smrtlink10), HGAP4²⁸ and Canu (v.1.6)²⁹ software. The alignment and analysis of the generated HiFi reads to the assembled genome were performed using the minimap2 (v2.15-r905) tool to evaluate genome coverage depth.

The assembled genome sequence of strain B115 has been uploaded and preserved in NCBI GenBank under accession number CP156682.

Genomic composition prediction

Genomic component prediction includes the prediction of coding genes, non-coding RNAs, repetitive sequences, Clustered Regularly Interspersed Short Palindromic Repeats (CRISPR), genomic islands, prophages, and secondary metabolite biosynthesis gene clusters (BGCs). Relevant coding genes were retrieved using the Glimmer (v3.02) programme. tRNA prediction of the B115 genome using tRNA prediction of the B115 genome using tRNAscan-SE (2.0.9), by RNAmmer (v1.2) for rRNA prediction, and prediction of potential RNAs (Excluding tRNA and rRNA) by matching genomes to the Rfam database via the cmscan programme of Infernal (v1.1.4).

The IslandPath-1.0.6 programme was used for the prediction of genomic islands, Phispy-4.2.19 software was used for the prediction of prophage structures in the genome, and Antibiotics and Secondary Metabolite Analysis Shell (antiSMASH) (v7.0, <https://antismash.secondarymetabolites.org/#!/start>) to predict BGCs in strain B115.

Comparative genomics

To explore the genetic differences between B115 and four other highly active *Bacillus* strains, as well as for strain identification of B115, we performed a comparative genome analysis of the genome-wide information of *B. velezensis* B115 and the other four highly active *Bacillus* strains using Mauve (v20150226)³⁰, with the use of *Staphylococcus aureus* NCTC 8325 as an exogenous species. Four strains of *Bacillus* including *B. velezensis* F42ZB (CP000560)²³, *B. velezensis* CBMB205 (CP011937)³¹, *B. amyloliquefaciens* GKTO4 (CP072120)³² and *B. velezensis* BR-01 (CP090150) (Unpublished). Genomic collinearity analysis was performed using blast (v2.11.0). Genomic information for all strains was downloaded from NCBI.

Functional annotation and analysis of genomes

The gene function annotation of B115 was performed based on Non-Redundant Protein Database (NR), Kyoto Encyclopedia of Gene and Genomes (KEGG)³³, Clusters of Orthologous Groups (COG), Gene Ontology (GO), and the Swiss-Prot databases for basic gene function annotation of B115. The database annotations for Swiss-Prot, KOG, NR, and KEGG were conducted employing the Blastp command of the Diamond software (v2.0.9.147) to align the genomic protein sequences with the respective databases.

GO function annotation was achieved utilizing the InterProScan software (v5.32-71.0)³⁴. Additionally, special functions of B115 were annotated based on The Comprehensive Antibiotic Research Database (CARD), Carbohydrate-Active Enzymes Database (CAZy), Pathogen Host Interactions Database (PHI), Virulence Factors of Pathogenic Bacteria (VFDB), Transporter Classification Database (TCDB), and restriction modification systems (RMS). The data annotation of CARD, PHI, VFDB, and TCDB was performed by comparing the predicted gene protein sequences with the respective databases using the Blastp parameter of the Diamond software (v2.0.9.147). The annotation of CAZymes was done using the HMMER-v3.3.2 annotation software, and the functional annotation of RMS was accomplished by blasting the predicted protein sequences with the REBASE database utilizing the Diamond software (v2.0.9.147).

Secondary metabolite analysis and identification

Analysis of metabolites in the fermentation broth of strain B115 using liquid chromatography tandem mass spectrometry (LC-MS/MS). Fermentation broth was prepared by inoculating single colonies of bacteria in LB liquid medium and incubating at 28 °C with 180 rpm shaking. The isolated strains were mixed in a 1:1 ratio (v/v) with 50% glycerol and stored at −80 °C. Following this, the samples were dispatched to Wuhan Fraser Genetic Information Co. Ltd. for untargeted metabolomics analysis. The experimental conditions were as follows:

The samples underwent analysis on a Waters ACQUITY Premier HSS T3 Column (2.1 mm × 100 mm, 1.8 µm) connected to an LC-30A ultra-high-performance liquid chromatograph (Japan) at a flow rate of 0.4 mL/min and a column temperature of 40 °C. Throughout the entire analysis process, the sample was consistently maintained at 4 °C in the autosampler. The chromatographic conditions included the utilization of two mobile phases: (A) 0.1% formic acid in water and (B) 0.1% formic acid in acetonitrile. The procedures were: 0–2 min, gradient 95–80% A, 2–5 min, gradient 80–40% A, 5–6 min, gradient 40–1% A, 6–7.5 min, 99% B, 7.5–7.6 min, gradient, 99–5% B, 7.6–10 min, 5% B. The chromatographic conditions were as follows.

Mass spectrometry analysis was performed using a TripleTOF 6600+ mass spectrometer (Foster City, CA, USA). The mass spectrometry conditions were as follows: electrospray ionization (ESI), ion source temperature: 550 °C, ion spray voltage: 5000 V, spray gas: 50 psi, curtain gas: 35 psi, auxiliary heated hot gas: 60 psi, declustering voltage: 60 V, MS1 collision energy: 10 V, MS2 collision energy: 30 V.

Identification of plant growth-promoting activity of B115

The isolated strain B115 was evaluated for siderophore and potassium solubility. To test the activity of siderophore of production, the production of siderophore was carried out on CAS medium, and after 7 days of incubation the aperture around the bacterial growth on the blue medium was observed, and the presence of an orange aperture indicated the production of siderophore³⁵. To evaluate the potassium solubilizing ability of strain B115, the potassium solubilization capacity was tested by incubation at 28 °C for 7 days following the method of Li et al.³⁶. Three replications were set up for each experiment.

Antagonistic activity against *F. oxysporum*

To assess the antifungal ability of B115, the inhibitory ability of B115 against *F. oxysporum* was evaluated on potato dextrose agar (PDA) using dual culture³⁷. The antagonistic ability of B115 against *F. oxysporum* was determined by comparing the radius size of *F. oxysporum* on plates inoculated with the pathogen alone (control plates), and on plates inoculated with the pathogen with B115 in double culture (experimental plates) and calculating the rate of inhibition based on the radius size. The experiment was set up with three replicates. Inhibition rate (100%) = (radius of control colony – radius of experimental colony)/radius of control colony × 100%. Colony radius size was measured with a ruler. The effect of volatile compounds (VOCs) produced by B115 on *F. oxysporum* was determined by a modified experimental method in which B115 and *F. oxysporum* strains were inoculated in two compartments of a 90-mm dichotomous Petri dish (with a partition in the middle separating the two strains, but with an upper space allowing gas exchange)³⁸. The plates were sealed using parafilm, incubated at 28 °C and observed for growth inhibition of pathogens. Plates inoculated only with fungal pathogens alone were used as control. The experiment was set up with three replications.

Result

Phylogenetic analysis of strain B115

Molecular characterization of B115 by 16S rDNA sequencing. The sequences were analyzed by NCBI BLAST online software to determine the species of isolated bacteria. Phylogenetic tree was performed using MEGA 11 software. The results of the analysis revealed that B115 showed the closest relationship to *B. velezensis* CBMB205 and *B. velezensis* FZB42, forming a distinct cluster. Hence, the initial classification of B115 as *B. velezensis* was confirmed (Fig. 1).

General characterisation of the genome of strain B115

In our exploration of the genomic profile of strain B115, we employed the PacBioSequel II sequencing platform. This endeavor yielded 41,145 CCS bases from a vast genetic landscape totaling 8,886,564,029 bp. The CCS sequences translated into a cumulative size of 434,487,669 bp, featuring an N50 length of 11,055 bp and a GC content of 45.84% (Table S1). The CCS sequences were circular assembled and the general characterisation of B115 showed a genome size of 4,220,774 bp (~4.2 Mb) (Fig. 2), with one plasmid region (Fig. S1). The examination predicted 4266 coding sequences, 87 tRNA genes, and 27 rRNA genes (16S–23S–5S rRNA), as delineated in Table S2. Furthermore, the scrutiny unveiled 10 CRISPRs, 5 gene islands totaling 251,948 bp with an average length of 50,389.60 per gene island, and 2 prophages, providing detailed insights in Tables S3–S4 and Fig. S2.

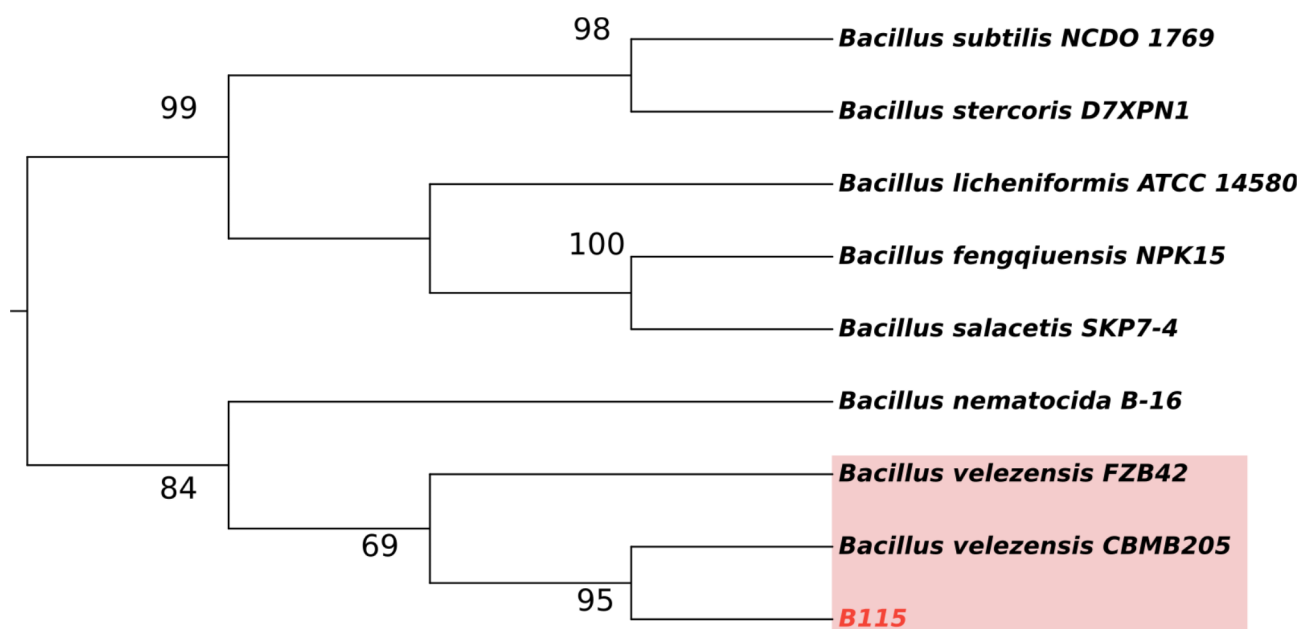


Fig. 1. Phylogenetic tree of the B115 strain based on 16S rDNA sequence alignments.

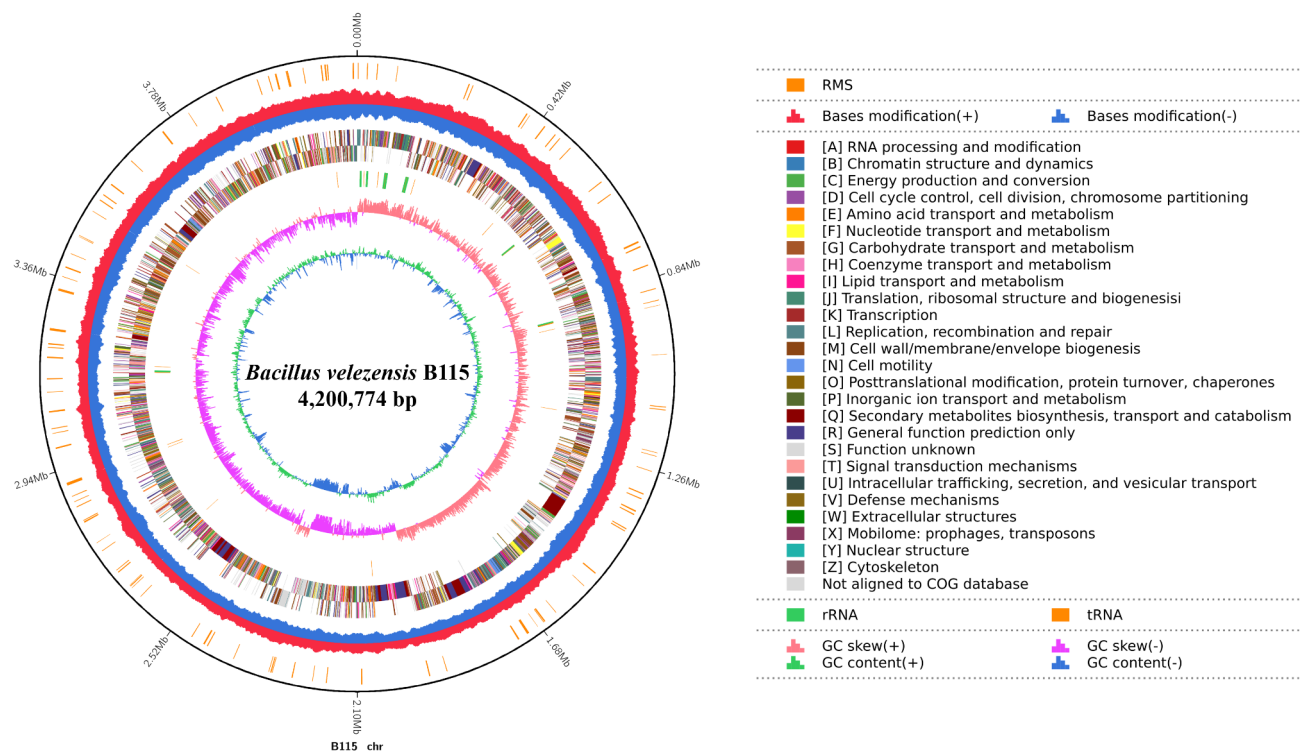


Fig. 2. Circular genome map of *B. velezensis* B115. From the innermost to the outermost: ring 1 for GC content, ring 2 for GC skew, ring 3 for distribution of rRNAs (green) and tRNAs (brown), ring 4 for COG classifications of protein-coding genes on the forward strand and reverse strand, ring 5 for restriction modification system, and ring 6 for genome size (black line).

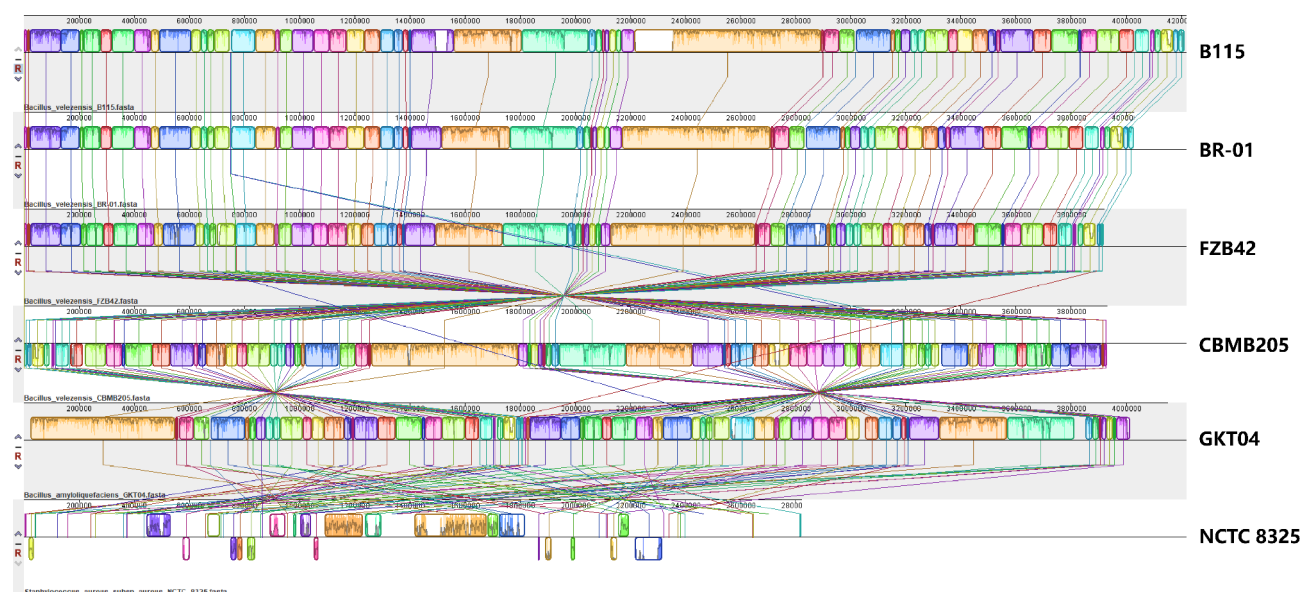


Fig. 3. Comparative genomic analysis of the genomes of B115 and four reference strains.

Comparative genome analysis

The analysis of genomic homozygosity revealed numerous inversions and rearrangements in the genomes of strain B115 compared to those of *B. velezensis* CBMB205 and *B. amyloliquefaciens* GKT04. Conversely, a significant level of homozygosity was observed with *B. velezensis* FZB42 and *B. velezensis* BR-01 strains (Fig. 3). Strain B115 was identified as *B. velezensis* B115 in combination with 16S rDNA phylogenetic analysis.

Functional annotation of the genome of strain B115

To obtain more comprehensive gene information, we performed gene function annotation. The genome sequences were aligned to five commonly used databases, matching 4266, 3664, 3212, 3178 and 2277 genes to sequences in the NR, Swiss-Prot, COG, KEGG and GO databases, respectively (Fig. S3). The GO information from the strain B115 genome was extracted using the InterProScan database³⁴. Through GO functional annotations, the identified proteins were categorized into three major groups: biological processes, cellular components, and molecular functions. The GO results revealed annotation of these proteins to 43 functional groups, comprising 25 biological processes, 3 cellular components, and 15 molecular functions. Within biological processes, the proteins were primarily associated with cellular processes (1834 genes), metabolic processes (1485 genes), and biological regulation (359 genes). In cellular components, proteins are involved in cellular anatomical entity (1972 genes), protein-containing complex (176 genes) and virion component (7 genes). In terms of molecular function, the proteins were mainly involved in catalytic activity (1720 genes), binding (1526 genes), and transporter activity (365 genes) (Fig. 4).

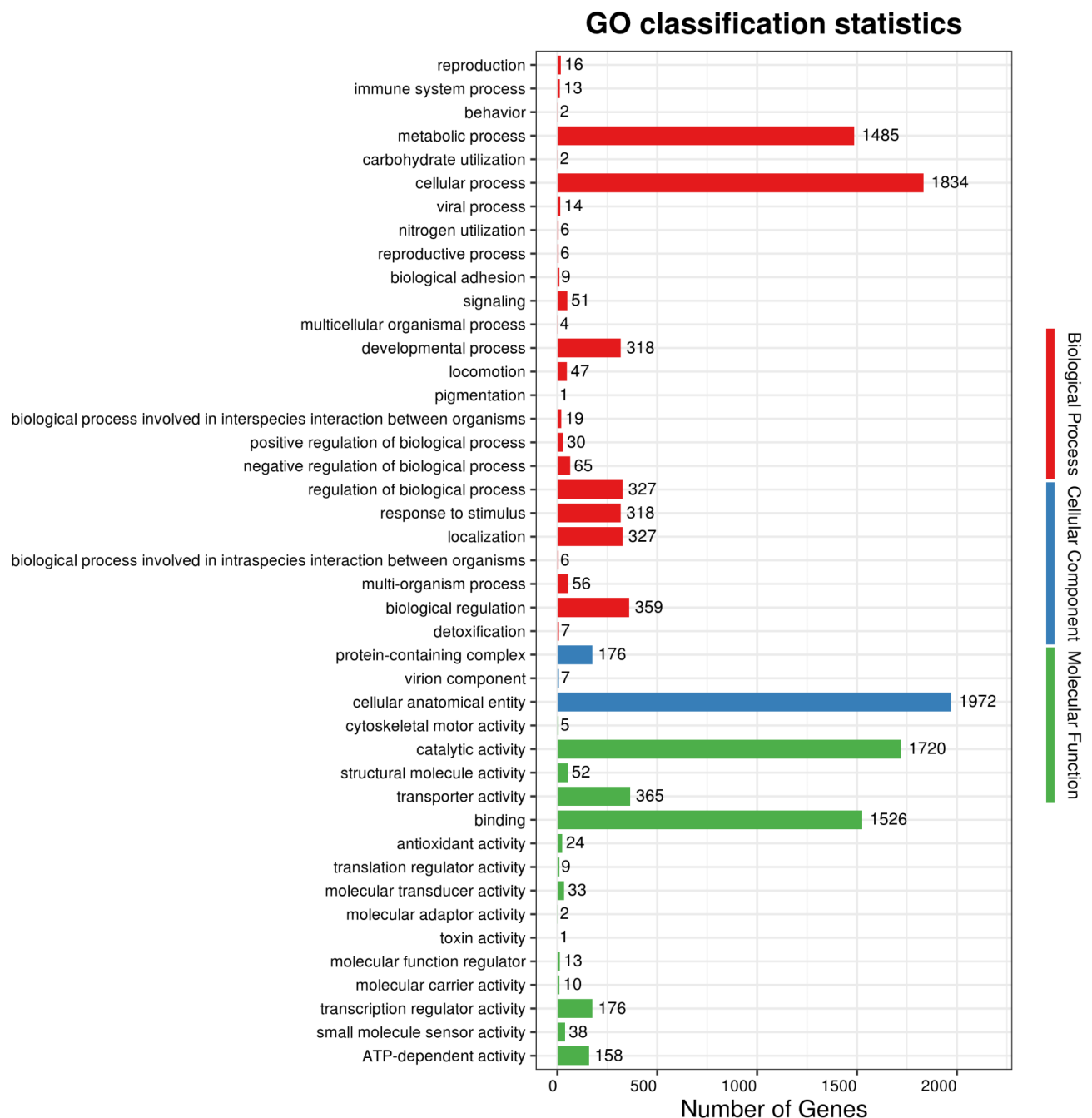


Fig. 4. GO annotation of *B. velezensis* B115.

Statistical analysis of genes involved in metabolic pathways in the genome sequence of *B. velezensis* B115 using KEGG analysis tool^{33,39,40}. The results indicated annotation of 40 KEGG pathways, categorized into six major groups: Cellular Process (163 genes), Environmental Information Processing (285 genes), Genetic Information Processing (179 genes), Human Disease (120 genes), Metabolism (1116 genes), and Organismal Systems (51 genes). Notably, the Carbohydrate Metabolic Pathway (241 genes) and Amino Acid Metabolic Pathway (206 genes) were the major enrichment pathways followed by Metabolism of Cofactors and Vitamins (165 genes) and Membrane Transport (166 genes) (Fig. 5A)^{33,39,40}.

The COG database predicted 3212 genes, classified into 24 categories, with transcription being the predominant functional category comprising 321 genes, representing 9.99% of all annotated protein sequences. Furthermore, 317 genes were linked to amino acid transport and metabolism, 293 genes to carbohydrate transport and metabolism, and 289 genes to general function prediction, accounting for 9.7%, 9.1%, and 9% of the total protein sequences, respectively. Remarkably, the annotation revealed 103 genes participating in secondary metabolite biosynthesis, transport, and catabolism (Fig. 5B).

Strain B115 underwent special functional annotation using CARD, CAZy, PHI, VFDB, TCDB, and RMS databases. A total of 1997 genes with special functions were identified, including 329 genes associated with CARD, 1070 genes associated with TCDB, 123 genes associated with RSM, 90 genes associated with CAZy, 1377 genes associated with PHI, and 700 genes associated with VFDB (Fig. 5C). In *B. velezensis* B115, a total of 90 CAZymes proteins were identified, with the highest percentage of glycoside hydrolases (GHs) class (44), followed by glycosyl transferases (GTs) (19) and carbohydrate esterases (CEs) (16) (Fig. S4).

In addition, a total of 1377 genes were identified in relation to pathogen-host interaction, with 919 genes associated with reduced virulence, followed by 436 genes associated with unaffected pathogenicity, and 26 of these PHI genes were predicted to be potential resistance genes. Protein BLAST analysis of the VFDB database identified a total of 700 genes associated with bacterial pathogenic virulence, and 188 of these secreted proteins were predicted to be involved in pathogen-host interactions (Fig. 5C).

Comparison of *B. velezensis* B115 with four other reference *Bacillus* strains

Bacillus is one of the most widely studied beneficial microorganisms at the inter-root level, and several commercial products belonging to the genus *Bacillus* are currently available for agricultural production⁴¹.

Research have studied *B. velezensis* FZB42 and found that it stimulates plant growth, synthesizes secondary metabolites, and inhibits soil-borne plant pathogens²³. Studies on *B. velezensis* N23 suggest that it may be a potential biocontrol agent in agricultural production and a source of further developed antimicrobial compounds⁴². The genome-wide information of *B. velezensis* B115 and four other highly active *Bacillus* strains, as outlined in Table 1. Comparative analysis of GC content showed that the GC content of B115 was not significantly different from the other four strains. Notably, the genome of *B. velezensis* B115 is larger than the other four genomes, at approximately 4.2 Mb. The number of genes encoding proteins in B115 was 4266, which was higher than the number of genes in *B. velezensis* FZB42 (3710), *B. velezensis* CBMB205 (3630), *B. amyloliquefaciens* GKT04 (3959) and *B. velezensis* BR-01 (3768) in terms of number of genes, suggesting that *B. velezensis* B115 has the potential to encode more and more complex proteins than other *Bacillus* strains.

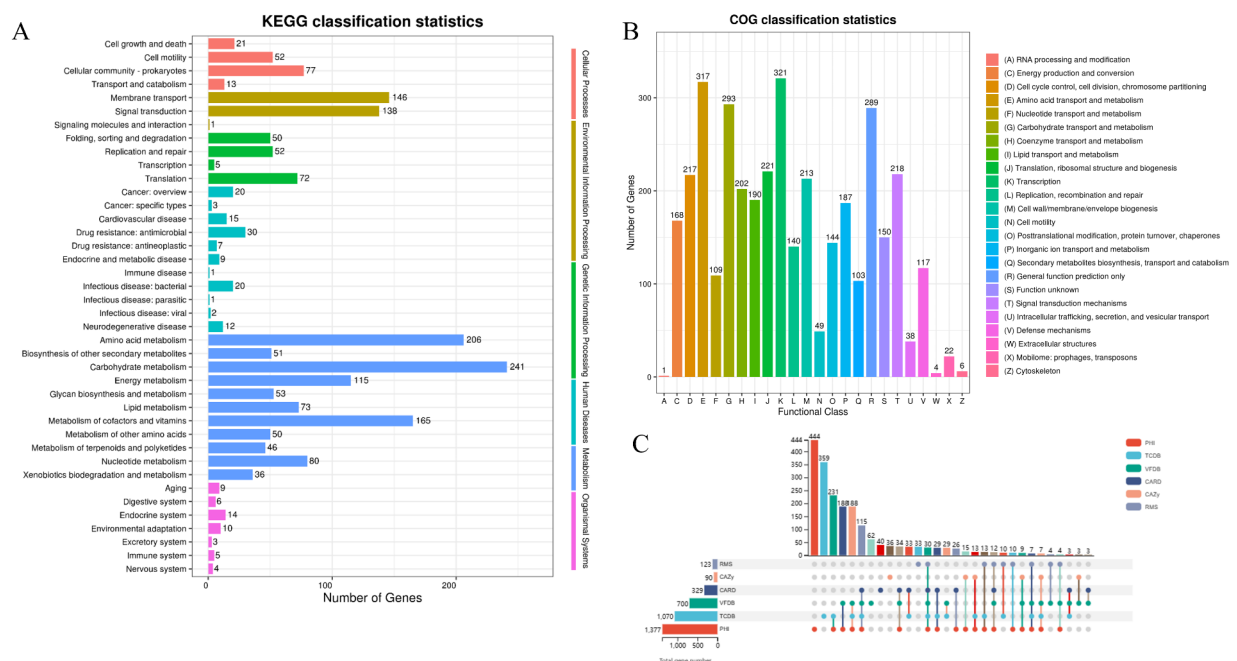


Fig. 5. (A): KEGG annotation of *B. velezensis* B115^{33,39,40}. (B): COG annotation of *B. velezensis* B115. (C): *B. velezensis* B115 Function-specific database shared and unique annotation analysis statistics charts.

Features	<i>B. velezensis</i> B115	<i>B. velezensis</i> FZB42	<i>B. velezensis</i> CBMB205	<i>B. amyloliquefaciens</i> GKT04	<i>B. velezensis</i> BR-01
Topology	Circular	Circular	Circular	Circular	Circular
Genome size	4,220,774 (~ 4.2 mb)	3,918,596 (~ 3.9 mb)	3,929,792 (~ 3.9 mb)	4,056,188 (~ 4.1 mb)	4,018,921 (~ 4.0 mb)
Coverage depth(X)	102.92 ×	100 ×	194.0 ×	400.0 ×	200 ×
GC content (%)	45.95	46.4	46.5	46.5	46.5
Total genes predicted	4349	3921	3800	4139	3943
CDS (with protein)	4266	3710	3630	3959	3768
tRNA	87	89	86	86	86
rRNA	27	29	27	27	27
Accession no	CP156682	CP000560	CP011937	CP072120	CP090150
Reference	This study	23	31	32	Unpublished

Table 1. Comparison of basic information of *B. velezensis* B115 with four other highly active *Bacillus* strains.

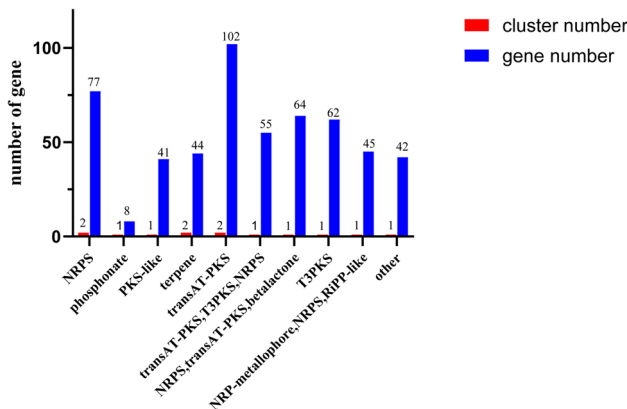


Fig. 6. Quantitative analysis of *B. velezensis* B115 secondary metabolite genes. NRPS nonribosomal peptide synthetase, PKS polyketide synthase, transAT-PKS trans-acyltransferase polyketide synthetases, T3PKS type III polyketide.

Secondary metabolite biosynthesis gene cluster in strain B115

Bacillus velezensis is recognized for its remarkable capability to produce secondary metabolites with antimicrobial properties. These secondary metabolites encompass lipopeptides (surfactin, fengycin, and bacillomycin D), polyketide compounds (macrolide, bacillaene, and difficidin or oxydifficidin), and peptides (plantazolicin, amylocyclin, and bacilysin). With the advancement of sequencing technology and the emergence of robust genome mining tools, researchers now have a wider array of avenues for investigating secondary metabolites. The antiSMASH expedites the annotation and analysis of secondary metabolite biosynthesis gene clusters, facilitating the estimation of compound types encoded by these clusters^{17,43}. Utilizing antiSMASH 7.0, a study on *B. velezensis* B115 successfully predicted 13 BGCs, including two NRPS clusters, one phosphonate cluster, one PKS-like cluster, two terpene clusters, two transAT-PKS clusters, one transAT-PKS, T3PKS, NRPS cluster, one NRPS, transAT-PKS, betalactone cluster, one T3PKS cluster, one NRP-metallophore, NRPS, RiPP-like cluster, and a cluster of genes of unknown function (referred to as others cluster) (Fig. 6).

Among these clusters, six clusters have 100% amino acid sequence homology with known gene clusters, including transAT-PKS (cluster 5 and cluster 10), transAT-PKS, T3PKS, NRPS (cluster 6), NRPS, transAT-PKS, betalactone (cluster 7), NRP-metallophore, NRPS, RiPP-like (cluster 11) and other (cluster 13). The above six clusters can synthesise macrolactin H, bacillaene, fengycin, difficidin, bacillibactin and bacilysin respectively (Table 2, Fig. 7). Within NRPS cluster 1, an 82% amino acid similarity is observed with the surface-active protein synthase gene cluster, while PKS-like cluster 3 shows a 7% amino acid similarity to the butirosin A/butirosin B synthase gene cluster. However, phosphonate (cluster 2), terpene (clusters 4 and 8), T3PKS (cluster 9), and NRPS (cluster 12) did not match any of the known gene clusters (Table 2, Fig. 7). The BGCs responsible for secondary metabolite synthesis in *B.velezensis* B115 was identified by genome mining, and detected clusters responsible for the synthesis of surfactin, butirosin A/butirosin B, macrolactin, bacillaene, fengycin, difficidin, bacillibactin, and bacilysin. The structures of these secondary metabolites are shown in Fig. 7. The structural composition of gene clusters 1 and 7 is shown in Fig. 7, which consist of lipopeptide synthesis genes such as surfactin and fengycin. The genome of *B. velezensis* B115 was analyzed using PRISM and the core genes were selected for PKS/NRPS analysis (Fig. 8). Utilizing PRISM, the core genes of *B. velezensis* B115 were analyzed for PKS/NRPS functions and the surfactin biosynthesis gene cluster was found to include Surf AA, Surf AB, and Surf AC. The fengycin biosynthesis gene cluster comprises nine genes. Furthermore, the B115 genome contained a cluster of surfactin synthesis genes, which was analyzed and found that the surfactin biosynthesis gene cluster of strain

Cluster number	Cluster name	From	To	Most similar known cluster		Similarity
1	NRPS	313,846	379,253	Surfactin	NRP:Lipopeptide	82%
2	Phosphonate	637,160	649,301	–	–	–
3	PKS-like	944,198	985,422	Butirosin A/Butirosin B	Saccharide	7%
4	Terpene	1,068,156	1,088,896	–	–	–
5	transAT-PKS	1,394,357	1,482,584	Macrolactin	Polyketide	100%
6	transAT-PKS, T3PKS, NRPS	1,750,869	1,860,971	Bacillaene	Polyketide + NRP	100%
7	NRPS, transAT-PKS, betalactone	1,926,678	2,064,508	Fengycin	NRP	100%
8	terpene	2,087,762	2,109,645	–	–	–
9	T3PKS	2,189,816	2,230,916	–	–	–
10	transAT-PKS	2,484,474	2,590,647	Difficidin	Polyketide	100%
11	NRP-metallophore, NRPS, RiPP-like	3,235,362	3,287,157	Bacillibactin	NRP	100%
12	NRPS	3,580,975	3,649,395	–	–	–
13	other	3,851,472	3,892,890	Bacilysin	Other	100%

Table 2. Cluster of genes encoding secondary metabolites in the genome of *B. velezensis* B115.

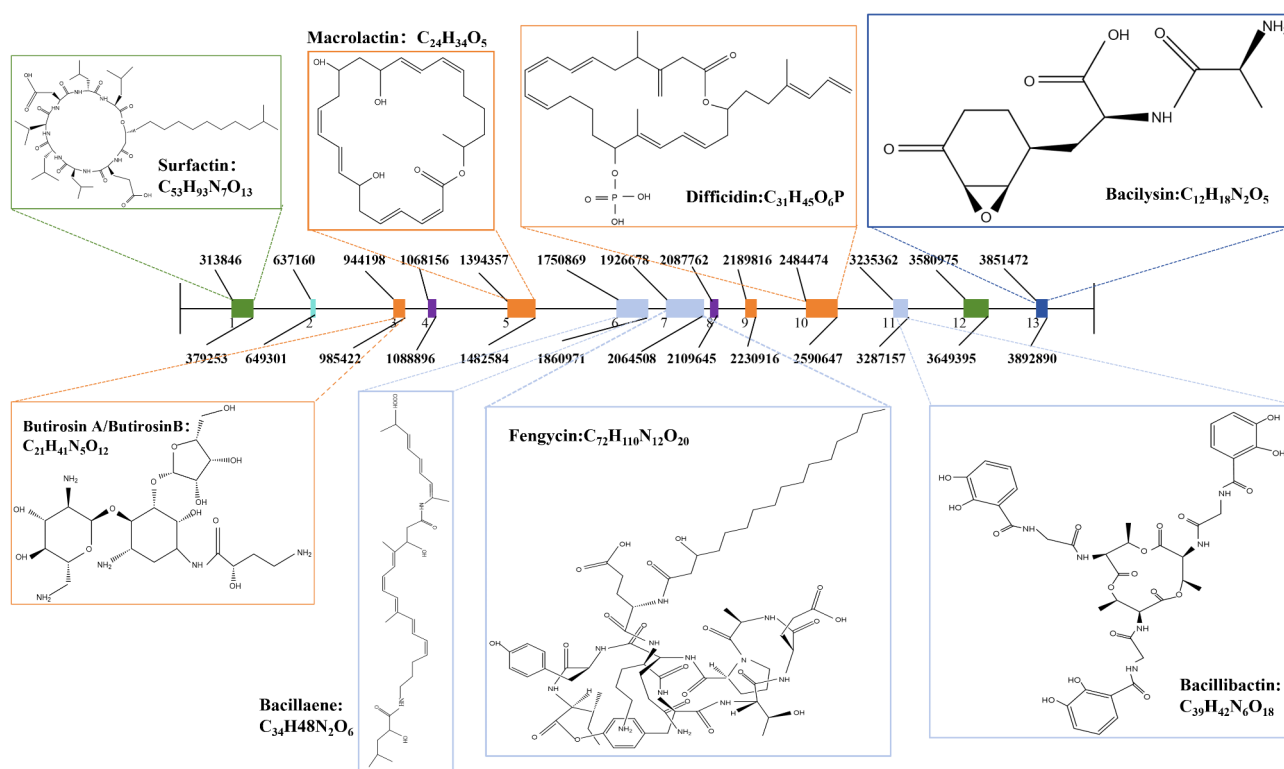


Fig. 7. Secondary metabolite gene clusters identified in *B. velezensis* B115 genome using antiSMASH software version 7.0.

B115 contained seven adenylated structural domains, named A1–A7. In addition, the potential substrates of A1–A7 were Glu, Leu, D-Leu, Val, Asp, D-Leu, and Leu, respectively (Fig. 8). Overall, the amino acid sequence of the surfactin produced by B115 may be Glu-Leu-D-Leu-Val-Asp-D-Leu-Leu.

Analysis of secondary metabolites in *B. velezensis* B115

The fermentation broth of B115 was tested and analyzed using non-targeted metabolomics techniques, and a total of 2318 identifiable metabolites were identified (Supplementary Table S1). Among the identifiable metabolites Amino acid and Its metabolites was the most abundant with 24.81% of all metabolites followed by Benzene and substituted derivatives (14.37%, Heterocyclic compounds (13.37%), Organic acid and Its derivatives (10.31%), Aldehyde, Ketones, Esters (7.33%), Hormones and hormone related compounds (3.49%), FA (3.24%) (Fig. S5).

Among the metabolites of *B. velezensis* strain B115, Corynebactin, Gamabufotalin, Pracinostat, Indoleacetic acid, (8)-Gingerol, Luteolin, Liquiritigenin and other antimicrobial, growth-promoting, antioxidant and antitumour metabolites were identified. antimicrobial, growth-promoting, antioxidant, and antitumour

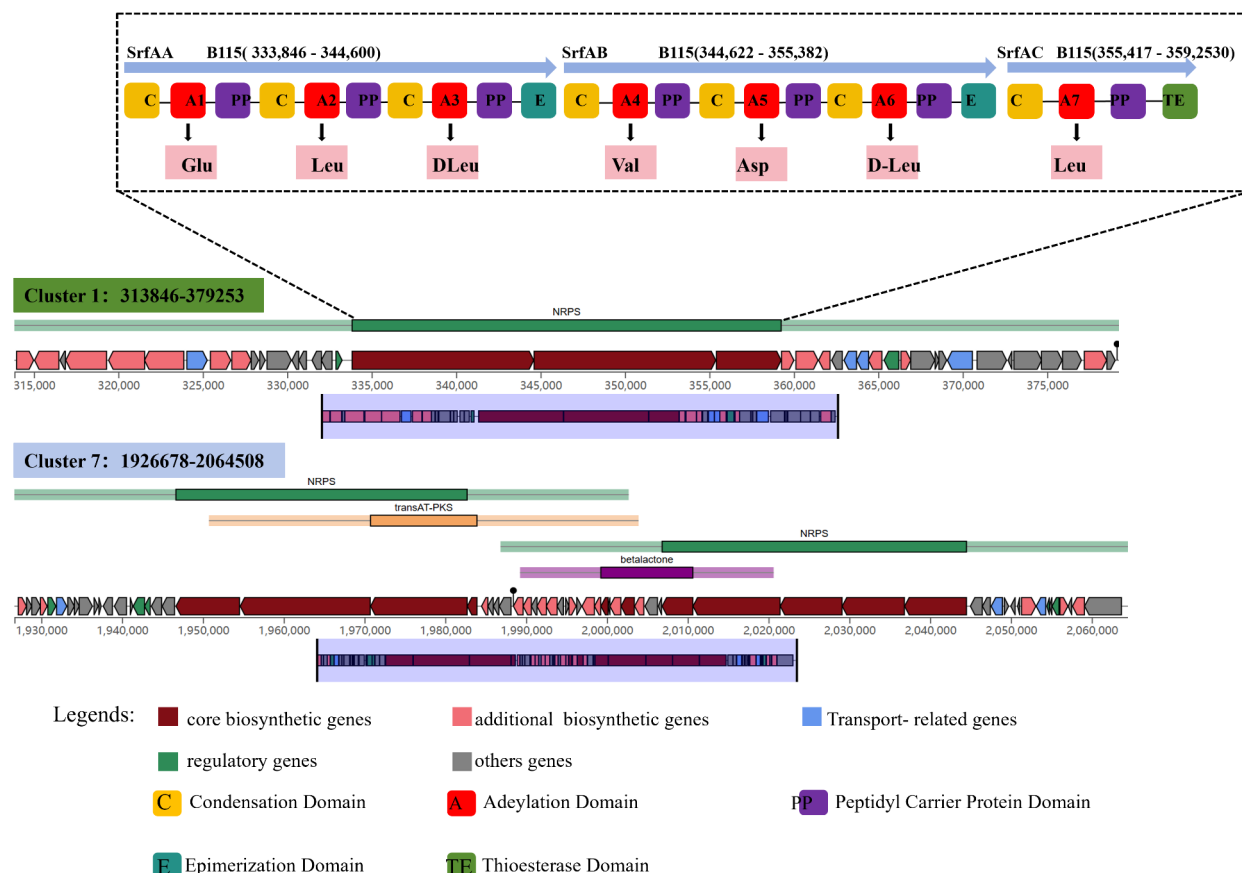


Fig. 8. Structural diagram of gene clusters 1 and 7 in *B. velezensis* B115. Clusters of potential secondary metabolite biosynthesis genes were predicted using antiSMASH. Genes with different functions were marked with different colour blocks as shown in the legend. Functional domains of genes related to surface activein synthesis were analysed using PKS/NRPS analysis, with abbreviations indicating the functions of the corresponding structural domains.

metabolites. Since strain B115 has many secondary metabolites of antimicrobial, antitumour, and immunological agents, it is presumed that strain B115 has antimicrobial, antitumour, and immunological agent effects.

Bacillus velezensis B115 growth-promoting properties of plants

To evaluate the growth-promoting activity of *B. velezensis* B115, the isolated B115 strain was evaluated for potassium and siderophore production. Figure S6c reveals that on the CAS plates inoculated with B115, an orange aperture emerged around the B115 strain, which suggests its capacity for siderophore production. Figure S6d showed that growth of strain B115 was observed on plates inoculated with B115, indicating its potassium solubilizing ability.

Antagonistic activity of B115 against *F. oxysporum*

Additionally, strain B115 was shown to inhibit *F. oxysporum* by plate antagonism assay (Fig. S6b). This was evidenced by the limitation of *F. oxysporum* growth after dual culture inoculation with B115 compared to inoculation with *F. oxysporum* alone (Fig. S6b). By calculating the inhibition rate, the inhibition is 73%, which is a strong inhibition ability. Experiments on the effect of VOCs produced by B115 on *F. oxysporum* showed that VOCs produced by strain B115 had an inhibitory effect on the growth of *F. oxysporum* as compared to petri dishes inoculated with *F. oxysporum* alone, as evidenced by the inhibitory effect on the colony size of *F. oxysporum*, which suggests that the VOCs produced by strain B115 (Fig. S7).

Discussion

Fusarium oxysporum is the main pathogenic fungus causing root-rot of *P. notoginseng*, in order to control this disease, some chemical pesticides are often used to prevent and control the disease, but the excessive use of chemical pesticides can easily lead to excessive pesticide residues and increased resistance of the pathogens, etc. Therefore, there is an urgent need for the development of safe and effective antifungal insecticides⁴⁴. Biological control methods have garnered attention due to their safety, environmental friendliness, and sustainability⁴⁵.

The escalating utilization of microorganisms, particularly bacteria, in agriculture underscores the demand for potent and effective BCAs⁴⁶.

The inter-root soil harbors a plethora of microorganisms, including Plant Growth-Promoting Rhizobacteria (PGPR) recognized for their roles in enhancing plant growth, instigating disease resistance, and managing soil-borne diseases. The application of PGPR can notably diminish the dependence on fertilizers and pesticides, thereby fostering environmental and human health benefits⁴⁷. *Bacillus* is a crucial member of PGPR, exhibits the ability to survive in harsh conditions by forming endospores and actively contributes to plant growth through phosphorus solubilization, nitrogen fixation, and the production of bioactive compounds like polyketides and lipopeptides that combat pathogens^{48,49}. *Bacillus velezensis* can secrete a variety of secondary metabolites to inhibit plant pathogens, which has a widerange of applications in agriculture and is one of the common biological control bacteria⁵⁰. In this study, a bacterium identified as strain B115, displaying growth-promoting and biocontrol properties, was isolated from the soil nearby healthy *P. notoginseng* plants in a continuous cropping area. This strain exhibited growth inhibition of *F. oxysporum* (Figs. S6b and S7) and showcased plant growth-promoting characteristics, including potassium solubilization and siderophore production. Phylogenetic analysis of the isolate based on 16S rDNA and comparative genomics identified it as *B. velezensis* B115. The whole genome of *B. velezensis* B115 showed a size of 4,200,774 bp (4.2 Mb) with a GC content of 45.95%, containing a plasmid region (Figs. 2 and S1). Although the variation in GC content compared to other *Bacillus* species is insignificant, B115's genome is notably larger, with 4349 predicted coding genes and 4,266 genes earmarked for protein encoding. The higher number of predicted genes in B115 than in other *Bacillus* strains suggests its potential for encoding a more diverse array of complex proteins.

At the molecular level, plant secondary metabolites play a crucial role in inhibiting pathogenic bacteria due to their antimicrobial properties²². Analysis of the secondary metabolite genes showed that *B. velezensis* B115 contains 13 BGCs that may synthesize eight secondary metabolites, including butirosin A/butirosin B, macrolactin, bacillaene, diffcadin, NRP (bacillibactin), bacilysin, surfactin, and fengycin, all of which have antimicrobial activity. Particularly, the non-ribosomal fengycin gene cluster not only showcases antimicrobial attributes but also stimulates systemic resistance in plants and fosters plant growth⁵¹. Moreover, the surfactin gene cluster demonstrates antimicrobial, antiviral, antitumor, and plant disease resistance properties⁵². The fermentation broth of B115 also contains Corynebactin, Gamabufotalin, Pracinostat, Indoleacetic acid, (8)-Gingerol, Luteolin, Liquiritigenin, and various other metabolites known for their antimicrobial, growth-promoting, antioxidant, and antitumor effects. Hence, it is hypothesized that strain B115 may amplify the resistance and antimicrobial efficacy of herbal medicines and crops in practical applications.

In addition to secondary metabolites, the genome analysis of *B. velezensis* B115 indicates its capacity to encode CAZymes. CAZymes play critical roles in immune responses, host–pathogen interactions, as well as in diseases affecting both humans and agriculture⁵³. Within B115, a comprehensive identification highlighted a total of 90 CAZymes proteins, primarily dominated by GHs with 44 enzymes, succeeded by GTs comprising 19 enzymes, and CEs with 16 enzymes. Furthermore, a special functional annotation of B115 uncovered genes associated with decreased virulence, potential drug resistance, bacterial pathogenicity, and interactions between pathogens and hosts.

These genes, which encode specific functions and are responsible for secreting secondary metabolic compounds in *B. velezensis* B115, endow the strain with significant value and play a vital role in promoting plant growth and maintaining plant health.

Conclusions

In this study, *B. velezensis* B115 isolated from healthy inter-root soils of a *P. notoginseng* continuous cropping site, showed robust antagonistic activity against *F. oxysporum*. B115 also has good plant growth-promoting capabilities. These findings suggest the broad spectrum of potential applications of *B. velezensis* B115 in both biological plant disease control and crop enhancement. Through whole genome sequencing and 16S rDNA analysis, the strain was identified as a member of the *B. velezensis* species. Its genome sequencing results showed that B115 contains a single circular chromosome of 4,200,774 bp in length with 4349 predicted genes and an average GC content of 45.95%. Genome mining identified 13 BGCs and 540 genes encoding secondary metabolites with predicted functions, including surfactin, and fengycin families. Furthermore, utilizing LC–MS/MS on the fermentation broth of *B. velezensis* B115, metabolites exhibiting antimicrobial, growth-promoting, antioxidant, and antitumor properties were identified. Leveraging the complete genome sequencing data, we conducted a comprehensive mining for genes associated with secondary metabolites in *B. velezensis* B115. The cumulative results strongly suggest that *B. velezensis* B115 holds great promise as a biocontrol agent for plant diseases and possesses a substantial capacity to produce diverse secondary metabolites.

In conclusion, strain B115 holds the potential to be developed into a plant growth promoter in the foreseeable future, to exert growth-promoting and plant disease-resistant effects. However, in determining the use of *B. velezensis* B115 as a plant growth promoter in agriculture, field trials are needed to explain its availability in the field. Furthermore, we predicted that *B. velezensis* B115 harbors significant potential to produce a great deal of secondary metabolites, and this work contributes to our understanding of its ability to biosynthesize secondary metabolites and lays the foundation for future exploitation of this valuable resource.

Data availability

The datasets presented in this study can be found in online repositories. All datasets supporting the conclusions of this article were included in the main manuscript file and the additional file. The raw data used in this study were deposited in NCBI Database with the 16S rDNA gene sequence was submitted with accession number PQ288536 and the draft genome with BioProject accession CP156682.

Received: 19 September 2024; Accepted: 26 February 2025

Published online: 28 March 2025

References

- Duan, L., Xiong, X., Hu, J., Liu, Y. & Wang, J. Efficacy and safety of oral *Panax notoginseng* saponins for unstable angina patients: A meta-analysis and systematic review. *Phytomedicine* **47**, 23–33. <https://doi.org/10.1016/j.phymed.2018.04.044> (2018).
- Chen, L., Yang, Y., Ge, J., Cui, X. & Xiong, Y. Study on the grading standard of *Panax notoginseng* seedlings. *J. Ginseng Res.* **42**, 208–217. <https://doi.org/10.1016/j.jgr.2017.03.006> (2018).
- Chen, W. et al. Whole-genome sequencing and analysis of the Chinese herbal plant *Panax notoginseng*. *Mol. Plant* **10**, 899–902. <https://doi.org/10.1016/j.molp.2017.02.010> (2017).
- Zhao, L. et al. Pesticide residues in soils planted with *Panax notoginseng* in south China, and their relationships in *Panax notoginseng* and soil. *Ecotoxicol. Environ. Saf.* **201**, 110783. <https://doi.org/10.1016/j.ecoenv.2020.110783> (2020).
- Lan, C. et al. First report of Sanqi (*Panax notoginseng*) root rot caused by *Pythium vexans* in China. *Plant Dis.* <https://doi.org/10.1094/pdis-04-22-0781-pdn> (2022).
- Dong, Y. et al. High concentrations of antagonistic bacterial strains from diseased sanqi ginseng rhizosphere suppressed *Fusarium* root rot. *Eur. J. Plant Pathol.* **163**, 143–153 (2022).
- Ning, K. et al. Genomic and transcriptomic analysis provide insights into root rot resistance in *Panax notoginseng*. *Front. Plant Sci.* **12**, 775019. <https://doi.org/10.3389/fpls.2021.775019> (2021).
- Zheng, Y. K. et al. Endophytic fungi harbored in *Panax notoginseng*: diversity and potential as biological control agents against host plant pathogens of root-rot disease. *J. Ginseng Res.* **41**, 353–360. <https://doi.org/10.1016/j.jgr.2016.07.005> (2017).
- Bonaterre, A. et al. Bacteria as biological control agents of plant diseases. *Microorganisms* **10**, 1759 (2022).
- Wang, C. et al. Isolation and characterization of *Bacillus velezensis* strain B19 for biocontrol of *Panax notoginseng* root rot. *Biol. Control* **185**, 105311. <https://doi.org/10.1016/j.biocontrol.2023.105311> (2023).
- Kimotho, R. N., Zheng, X., Li, F., Chen, Y. & Li, X. A potent endophytic fungus *Purpureocillium lilacinum* YZ1 protects against *Fusarium* infection in field-grown wheat. *New Phytol.* **243**, 1899–1916. <https://doi.org/10.1111/nph.19935> (2024).
- Chen, Z., Wang, Z. & Xu, W. *Bacillus velezensis* WB induces systemic resistance in watermelon against *Fusarium* wilt. *Pest Manag. Sci.* **80**, 1423–1434. <https://doi.org/10.1002/ps.7873> (2024).
- Lim, S. B. Y. et al. Genome sequence of *Bacillus velezensis* SGAir0473, isolated from tropical air collected in Singapore. *Genome Announc.* **6**, e00642. <https://doi.org/10.1128/genomeA.00642-18> (2018).
- Ye, M. et al. Characteristics and application of a novel species of *Bacillus*: *Bacillus velezensis*. *ACS Chem. Biol.* **13**, 500–505. <https://doi.org/10.1021/acscchembio.7b00874> (2018).
- Khalid, F. et al. Potential of *Bacillus velezensis* as a probiotic in animal feed: A review. *J. Microbiol.* **59**, 627–633. <https://doi.org/10.1007/s12275-021-1161-1> (2021).
- Wang, J. et al. Complete genome sequencing of *Bacillus velezensis* WRN014, and comparison with genome sequences of other *Bacillus velezensis* strains. *J. Microbiol. Biotechnol.* **29**, 794–808. <https://doi.org/10.4014/jmb.1901.01040> (2019).
- Zhou, H. et al. Efficacy of plant growth-promoting bacteria *Bacillus cereus* YN917 for biocontrol of rice blast. *Front. Microbiol.* **12**, 684888. <https://doi.org/10.3389/fmicb.2021.684888> (2021).
- Xu, Y. et al. Macrolactin XY, a macrolactin antibiotic from marine-derived *Bacillus subtilis* sp. 18. *Mar. Drugs* **22**, 331. <https://doi.org/10.3390/md22080331> (2024).
- Zhao, L. et al. Biochar increases *Panax notoginseng*'s survival under continuous cropping by improving soil properties and microbial diversity. *Sci. Total Environ.* **850**, 157990. <https://doi.org/10.1016/j.scitotenv.2022.157990> (2022).
- Tan, Y. et al. Diversity and composition of rhizospheric soil and root endogenous bacteria in *Panax notoginseng* during continuous cropping practices. *J. Basic Microbiol.* **57**, 337–344. <https://doi.org/10.1002/jobm.201600464> (2017).
- Shen, Y. et al. Whole genome sequencing provides evidence for *Bacillus velezensis* SH-1471 as a beneficial rhizosphere bacterium in plants. *Sci. Rep.* **13**, 20929. <https://doi.org/10.1038/s41598-023-48171-9> (2023).
- Salwan, R. & Sharma, V. Genome wide underpinning of antagonistic and plant beneficial attributes of *Bacillus* sp. SBA12. *Genomics* **112**, 2894–2902. <https://doi.org/10.1016/j.ygeno.2020.03.029> (2020).
- Chen, X. H. et al. Comparative analysis of the complete genome sequence of the plant growth-promoting bacterium *Bacillus amyloliquefaciens* FZB42. *Nat. Biotechnol.* **25**, 1007–1014. <https://doi.org/10.1038/nbt1325> (2007).
- Erlacher, A., Cardinale, M., Grosch, R., Grube, M. & Berg, G. The impact of the pathogen *Rhizoctonia solani* and its beneficial counterpart *Bacillus amyloliquefaciens* on the indigenous lettuce microbiome. *Front. Microbiol.* **5**, 175. <https://doi.org/10.3389/fmicb.2014.00175> (2014).
- Chowdhury, S. P., Hartmann, A., Gao, X. & Borris, R. Biocontrol mechanism by root-associated *Bacillus amyloliquefaciens* FZB42—A review. *Front. Microbiol.* **6**, 780. <https://doi.org/10.3389/fmicb.2015.00780> (2015).
- Wang, L. et al. Genomic and metabolomic insights into the antimicrobial compounds and plant growth-promoting potential of *Bacillus velezensis* Q-426. *BMC Genom.* **24**, 589. <https://doi.org/10.1186/s12864-023-09662-1> (2023).
- Song, Y. et al. Effect of endophytic fungi on the host plant growth, expression of expansin gene and flavonoid content in *Tetragonia hemsleyana* Diels & Gilg ex Diels. *Plant Soil* **417**, 393–402. <https://doi.org/10.1007/s1104-017-3266-1> (2017).
- Chin, C. S. et al. Nonhybrid, finished microbial genome assemblies from long-read SMRT sequencing data. *Nat. Methods* **10**, 563–569. <https://doi.org/10.1038/nmeth.2474> (2013).
- Chaisson, M. J. & Tesler, G. Mapping single molecule sequencing reads using basic local alignment with successive refinement (BLASR): Application and theory. *BMC Bioinform.* **13**, 238. <https://doi.org/10.1186/1471-2105-13-238> (2012).
- Darling, A. C., Mau, B., Blattner, F. R. & Perna, N. T. Mauve: Multiple alignment of conserved genomic sequence with rearrangements. *Genome Res.* **14**, 1394–1403. <https://doi.org/10.1101/gr.2289704> (2004).
- Hwangbo, K. et al. Complete genome sequence of *Bacillus velezensis* CBMB205, a phosphatase-solubilizing bacterium isolated from the rhizosphere of rice in the Republic of Korea. *Genome Announc.* **4**, 10–1128. <https://doi.org/10.1128/genomeA.00654-16> (2016).
- Tian, D. et al. Antifungal mechanism of *Bacillus amyloliquefaciens* strain GKT04 against *Fusarium* wilt revealed using genomic and transcriptomic analyses. *Microbiologyopen* **10**, e1192. <https://doi.org/10.1002/mbo3.1192> (2021).
- Kanehisa, M. & Goto, S. KEGG: Kyoto encyclopedia of genes and genomes. *Nucleic Acids Res.* **28**, 27–30. <https://doi.org/10.1093/nar/28.1.27> (2000).
- Ashburner, M. et al. Gene ontology: Tool for the unification of biology. The Gene Ontology Consortium. *Nat. Genet.* **25**, 25–29. <https://doi.org/10.1038/75556> (2000).
- Cavite, H. J. M., Mactal, A. G., Evangelista, E. V. & Cruz, J. A. Growth and yield response of upland rice to application of plant growth-promoting rhizobacteria. *J. Plant Growth Regul.* **40**, 494–508 (2021).
- Li, J. et al. *Pseudomonas* species isolated from tobacco seed promote root growth and reduce lead contents in *Nicotiana glauca* K326. *Can. J. Microbiol.* **65**, 214–223. <https://doi.org/10.1139/cjm-2018-0434> (2019).
- Sharma, V. & Shanmugam, V. Purification and characterization of an extracellular 24 kDa chitinase from the mycoparasitic fungus *Trichoderma saturnisporum*. *J. Basic Microbiol.* **52**, 324–331. <https://doi.org/10.1002/jobm.201100145> (2012).
- Salwan, R., Sharma, V., Sharma, A. & Singh, A. Molecular imprints of plant beneficial *Streptomyces* sp. AC30 and AC40 reveal differential capabilities and strategies to counter environmental stresses. *Microbiol. Res.* **235**, 126449. <https://doi.org/10.1016/j.micres.2020.126449> (2020).

39. Kanehisa, M. Toward understanding the origin and evolution of cellular organisms. *Protein Sci.* **28**, 1947–1951. <https://doi.org/10.1002/pro.3715> (2019).
40. Kanehisa, M., Furumichi, M., Sato, Y., Kawashima, M. & Ishiguro-Watanabe, M. KEGG for taxonomy-based analysis of pathways and genomes. *Nucleic Acids Res.* **51**, D587–d592. <https://doi.org/10.1093/nar/gkac963> (2023).
41. Mowafy, A. M., Fawzy, M. M., Gebreil, A. & Elsayed, A. Endophytic *Bacillus*, *Enterobacter*, and *Klebsiella* enhance the growth and yield of maize. *Acta Agric. Scand. Sect. B Soil Plant Sci.* **71**, 237–246 (2021).
42. Yang, P. et al. Genome sequencing and characterization of *Bacillus velezensis* N23 as biocontrol agent against plant pathogens. *Microorganisms* **12**, 294. <https://doi.org/10.3390/microorganisms12020294> (2024).
43. Blin, K. et al. antiSMASH 7.0: New and improved predictions for detection, regulation, chemical structures and visualisation. *Nucleic Acids Res.* **51**, W46–w50. <https://doi.org/10.1093/nar/gkad344> (2023).
44. Nie, H. et al. *Foeniculum vulgare* essential oil nanoemulsion inhibits *Fusarium oxysporum* causing *Panax notoginseng* root-rot disease. *J. Ginseng Res.* **48**, 236–244. <https://doi.org/10.1016/j.jgr.2023.12.002> (2024).
45. Wei, J. et al. Biocontrol mechanisms of *Bacillus velezensis* against *Fusarium oxysporum* from *Panax ginseng*. *Biol. Control* **182**, 105222 (2023).
46. Tsalgatidou, P. C. et al. Integrated genomic and metabolomic analysis illuminates key secreted metabolites produced by the novel endophyte *Bacillus halotolerans* Cal.1.30 involved in diverse biological control activities. *Microorganisms* **10**, 399. <https://doi.org/10.3390/microorganisms10020399> (2022).
47. Hakim, S. et al. In *Frontiers in Sustainable Food Systems*.
48. Li, X. et al. Genomic and transcriptomic analyses of *Bacillus methylotrophicus* NJ13 reveal a molecular response strategy combating *Ilyonectria robusta* causing ginseng rusty root rot. *Biol. Control* **172**, 104972. <https://doi.org/10.1016/j.biocontrol.2022.104972> (2022).
49. Li, Z., Song, C., Yi, Y. & Kuipers, O. P. Characterization of plant growth-promoting rhizobacteria from perennial ryegrass and genome mining of novel antimicrobial gene clusters. *BMC Genom.* **21**, 157. <https://doi.org/10.1186/s12864-020-6563-7> (2020).
50. Glaeser, S. P. & Kämpfer, P. Multilocus sequence analysis (MLSA) in prokaryotic taxonomy. *Syst. Appl. Microbiol.* **38**, 237–245. <https://doi.org/10.1016/j.syapm.2015.03.007> (2015).
51. Zhang, P., Yin, Y. & Wen, J. Fermentation optimization and metabolomic analysis of a *Bacillus subtilis* co-culture system for fengycin production from mixed sugars. *Biochem. Eng. J.* **209**, 109406. <https://doi.org/10.1016/j.bej.2024.109406> (2024).
52. Qiao, J. et al. Research advances in the identification of regulatory mechanisms of surfactin production by *Bacillus*: A review. *Microb. Cell Fact.* **23**, 100. <https://doi.org/10.1186/s12934-024-02372-7> (2024).
53. López-Sánchez, R. et al. Metagenomic analysis of carbohydrate-active enzymes and their contribution to marine sediment biodiversity. *World J. Microbiol. Biotechnol.* **40**, 95. <https://doi.org/10.1007/s11274-024-03884-5> (2024).

Acknowledgements

This study was financially supported by the Key projects of Yunnan provincial natural fund (202201AS070064), the National Key Research and Development (2021YFD1601003, the Development and Application of Quality Standards for Decomposed Agricultural Fertiliser for Tobacco Use (KMYC202313), the Cigar tobacco quality control evaluation system research and application (No: HYHH2021YL01), the Research and application of personalized cigarette products (2023CP02), the Project of The Sino-Vietnamese International Joint Laboratory for Characteristic & Cash Crops Green Development of Yunnan Province (202403AP140013).

Author contributions

B.Z. and T.L. conceptualize the experiment and project management. J.L.C., Y.Z.F., and J.C.M. wrote the original manuscript. Q.Z., B.C., and Y.M.D. revised part of the paper and completed some experiments. D.J.L., J.L.Y., X.M.D. collated data and formal analysis. L.Q.Z., Z.H.L., Z.L., and Y.Y. review and editing. All authors reviewed the manuscript.

Declarations

Competing interests

The authors declare no competing interests.

Additional information

Supplementary Information The online version contains supplementary material available at <https://doi.org/10.1038/s41598-025-92322-z>.

Correspondence and requests for materials should be addressed to J.C., B.Z. or T.L.

Reprints and permissions information is available at www.nature.com/reprints.

Publisher's note Springer Nature remains neutral with regard to jurisdictional claims in published maps and institutional affiliations.

Open Access This article is licensed under a Creative Commons Attribution-NonCommercial-NoDerivatives 4.0 International License, which permits any non-commercial use, sharing, distribution and reproduction in any medium or format, as long as you give appropriate credit to the original author(s) and the source, provide a link to the Creative Commons licence, and indicate if you modified the licensed material. You do not have permission under this licence to share adapted material derived from this article or parts of it. The images or other third party material in this article are included in the article's Creative Commons licence, unless indicated otherwise in a credit line to the material. If material is not included in the article's Creative Commons licence and your intended use is not permitted by statutory regulation or exceeds the permitted use, you will need to obtain permission directly from the copyright holder. To view a copy of this licence, visit <http://creativecommons.org/licenses/by-nc-nd/4.0/>.

© The Author(s) 2025